

Hybrid nonlinear control of a tall tower with a pendulum absorber

Diego Orlando^a and Paulo B. Gonçalves*

*Department of Civil Engineering, Pontifical Catholic University of Rio de Janeiro,
PUC-Rio, Rio de Janeiro, RJ, 22451-900, Brazil*

(Received July 5, 2012, Revised March 2, 2013, Accepted March 29, 2013)

Abstract. Pendulums can be used as passive vibration control devices in several structures and machines. In the present work, the nonlinear behavior of a pendulum-tower system is studied. The tower is modeled as a bar with variable cross-section with concentrated masses. First, the vibration modes and frequencies of the tower are obtained analytically. The primary structure and absorber together constitute a coupled system which is discretized as a two degrees of freedom nonlinear system, using the normalized eigenfunctions and the Rayleigh-Ritz method. The analysis shows the influence of the geometric nonlinearity of the pendulum absorber on the response of the tower. A parametric analysis also shows that, with an appropriate choice of the absorber parameters, a pendulum can decrease the vibration amplitudes of the tower in the main resonance region. The results also show that the pendulum nonlinearity cannot be neglected in this type of problem, leading to multiplicity of solutions, dynamic jumps and instability. In order to improve the effectiveness of the control during the transient response, a hybrid control system is suggested. The added control force is implemented as a non-linear variable stiffness device based on position and velocity feedback. The obtained results show that this strategy of nonlinear control is attractive, has a good potential and can be used to minimize the response of slender structures under various types of excitation.

Keywords: tower; nonlinear oscillations; passive control; pendulum absorber; hybrid control; variable stiffness spring

1. Introduction

High-rise buildings, free standing towers, chimneys, smoke or ventilation stacks and tall poles are vulnerable, due to its height and slenderness, to the occurrence of extreme vibrations caused by environmental loads, such as wind and earthquakes. The action of the wind is of utmost importance in the design of tall structures, since it generates flexural vibrations, causing large displacements and rotations in the top of the structure. These vibrations usually are caused by vortex shedding. In towers, the worst case occurs when vortex-shedding frequencies coincide with the frequency of the first vibration mode of the tower (Korenev and Reznikov 1993). An alternative to minimize these vibrations, widely studied in the last decades, is the use of structural vibration control. It is capable of absorbing and dissipating part of the vibratory energy of the

*Corresponding author, Professor, E-mail: paulo@puc-rio.br

^aPh.D., E-mail: dgorlando@gmail.com

system, reducing in this way the response of the main structure. The endeavor to minimize vibrations is motivated by necessity to assure the safety of structures, eliminate dangerous fatigue stresses, serviceability, should they be used for the installation of sensitive measuring equipment, and human health or comfort, which can be impaired by excessive movements. Basic concepts, experiments and practical applications of these control devices are found in Soong and Dargush (1997), amongst others. For an extensive monograph dealing with dynamic absorbers, see Korenev and Reznikov (1993).

A control device increasingly used in practical applications is the tuned mass dampers (TMDs). A tuned mass damper is a classical passive controller of excessive vibrations around the resonant frequencies of lightly damped structures (Den Hartog 1985). This type of structural control has shown to be robust, trustworthy and economic. Therefore, the TMDs have become object of the attention of researchers and engineers worldwide. The TMD is usually designed to bring the amplitude of the resonance peak to its lowest possible value, so that smaller amplifications of the response of the structure in the neighborhood of the main resonance frequency can be reached (Soong and Dargush 1997, Den Hartog 1985). The magnitude of the control forces depends only on its physical properties of mass, stiffness and damping. However there are some limitations in the use of this technology, since the passive devices are designed to work efficiently within a small frequency range. One passive control device proposed in literature is the pendulum absorber.

Mustafa and Ertas (1995) investigated the dynamic response of a large flexible beam with a tip mass–pendulum system. The system is proposed as a conceptualization of a vibration-absorbing device for large flexible structures with tip appendages. Later, Ertas *et al.* (2000) studied the effectiveness of pendulum-type passive vibration absorber attached to a primary structure with a varying orientation about a vertical plane. Collette (1998) studied numerically and experimentally the vibration control capability of a combined tuned absorber and pendulum impact damper under a random excitation.

Cicek (2002) analyzed experimentally the response of this system to a wide-band random excitation. Gerges and Vickery (2003) conducted an extensive experimental study of a single-degree-of-freedom system with a nonlinear pendulum-type TMD and compared its frequency response functions to those of equivalent optimized linear TMDs. Battista *et al.* (2003) studied the efficiency of a non-linear pendulum-like damper on the dynamic behavior and stability of transmission line towers under wind forces. The analysis of the orientation effect of non-linear flexible systems on performance of the pendulum absorber was also studied by Yaman and Sen (2004). Pendulum absorbers have already been used in several structures such as the Cristal Tower in Tokyo and the Taipei 101 super-tall building (Nagase and Hisatoku 1992, Li *et al.* 2011, Kourakis 2007).

Pendulum absorbers have also been used as auto parametric vibration absorbers. Vyas and Bajaj (2001) analyzed the dynamics of a resonantly excited single-degree-of-freedom linear system coupled to an array of non-linear auto parametric vibration absorbers (pendulums) and showed that the frequency interval of the unstable single-mode response, or the absorber bandwidth, can be enlarged compared to that of a single pendulum absorber by adjusting the internal mistuning of the pendulums. Warminski and Kecik (2009) studied the instabilities in the main parametric resonance area of a nonlinear mechanical oscillator with an attached damped pendulum. The analytical results are verified by numerical simulations and experimental tests. Regions of regular oscillations, chaotic motions, and full rotation of the pendulum are confirmed experimentally. Macias-Cundapi *et al.* (2008) dealt with the passive/active vibration control problem for damped Duffing systems, using a nonlinear pendulum-type vibration absorber. Wu

(Wu 2009, Wu *et al.* 2011) proposed an active spatial pendulum vibration absorber with a spinning support for neutralization of vertical excitations. The frequency of the absorber is dynamically tuned by varying its rotational speed. Náprstek and Fischer (2009) investigated the auto-parametric semi-trivial and post-critical response of a spherical pendulum damper modeled as a two degree of freedom strongly non-linear auto-parametric system. The excitation is considered to be horizontal and harmonically variable in time.

The characteristic frequency of a simple pendulum is a function of the suspension length and gravity only. In some applications the tuned pendulum may require extremely long or short suspensions. In such cases, it is possible to replace the classical pendulum by similar devices. Pirner (2002) described the theory, experiments and practical application of the ball vibration absorber for horizontal movement, as well as its efficiency in comparison with that of the pendulum absorber. Fischer (2007) compared the effect of pendulum, ball and sloshing liquid absorbers and assesses the effectiveness of each of them. Matta and De Stefano (2009) evaluated the performance of circular and cycloid rolling-pendulum TMD type for the seismic protection of buildings, a configuration characterized by mass-independent natural period, in order to illustrate their respective advantages as well as the drawbacks inherent in their non-linear behavior.

Another way of controlling the dynamics of slender structures proposed in literature is the switched stiffness approach. Nitzsche *et al.* (1999, 2004) proposed the so called smart spring concept to actively control combinations of dynamic impedance characteristics of a structure, such as the stiffness, damping, and effective mass to suppress vibration in an indirect manner, without requiring large forces and deflections simultaneously. Ramaratnam *et al.* (2004) suggested a semi-active vibration control device using piezoelectric-based switched stiffness. Later, Ramaratnam and Jalili (2006) proposed a semi-active structural vibration control based on switching the system equivalent stiffness between two distinct values. This vibration control method leads to change in the stored potential energy, which results in reduced total energy of the system. The switched stiffness can be implemented using a bi-stiffness spring setting, with the resulting relay-type control logic based on the position and velocity feedback. A heuristic control law is used to switch the stiffness values through a hard switching or on-off (relay) control (Clark 2000). Wu *et al.* (2005) demonstrated that active variable stiffness systems may be effective for response control of building structures subjected to earthquake excitations. This control law exhibits strong nonlinearity. Nagarajaiah and Varadarajan (2005) presented a short time Fourier transform algorithm for wind response control of buildings with variable stiffness TMD. Winthrop *et al.* (2005) compared several variable stiffness devices found in the literature in terms of their ability to change stiffness. Azadi *et al.* (2009, 2011) presented the concept of variable stiffness elements based on antagonistic forces (prestress) in cable-driven mechanisms and discuss the challenges of implementing such device in practical applications. González Rodríguez *et al.* (2011) advocated an adjustable-stiffness actuator composed of two antagonistic non-linear springs, which consists of two pairs of leaf springs working in bending conditions under large displacements. Owing to this geometric non-linearity, the global stiffness of the actuator can be adjusted by modifying the shape of the leaf springs.

The hybrid control approaches combine active controllers with passive devices. The active portion of a hybrid system requires much less power than a similar active system, while providing better structural response than the passive system alone (Oueini *et al.* 1999, Gonçalves and Orlando 2007). Spencer and Nagarajaiah (2003), in a review article, present a large number of existing tall buildings and bridges where hybrid control systems have been employed due to its good performance.

Here a hybrid control approach is proposed based on the simultaneous use of a nonlinear pendulum absorber with an active variable stiffness device. The active force is based on the basic ideas of the switched stiffness approach (Wu *et al.* 2005). The tower is modeled as a bar with constant or variable cross-section (Korenev and Reznikov 1993, Qiusheng *et al.* 1994) and concentrated masses. First, the vibration modes and frequencies of the tower are obtained analytically. Using these vibration modes as interpolating functions, the natural frequencies and modes of the column-pendulum system are obtained by the Rayleigh-Ritz method. For a pendulum tuned to the lowest frequency of the tower (first flexural mode), only the two first vibration modes and frequencies of the tower-pendulum system are important, since the subsequent frequencies of the cantilevered tower are much higher than the first ones. So, using these two vibration modes, a simplified two degrees of freedom nonlinear system is obtained, which is a useful tool in early design stages. The resulting equations are highly nonlinear due to the variable stiffness spring and the inertial and geometric nonlinearities of the moving pendulum. These equations are solved numerically using the Runge-Kutta method. Floquet theory is used in the stability analysis of the responses. In order to study the non-linear behavior of the controlled system, several numerical strategies were used to obtain Poincaré maps, stable and unstable fixed points, bifurcation diagrams and basins of attraction.

2. Formulation of the problem

The tower is modeled as a clamped-free column with variable cross-section. Fig. 1 shows the tower and pendulum geometric parameters used in the problem formulation. Platforms, antennas and other equipment can be modeled as discrete masses along the tower, as shown in Fig. 1. The pendulum is considered as a discrete element.

The behavior of the column-pendulum system shown in Fig. 1 is described by the following Lagrange function (Orlando 2006)

$$\begin{aligned}
 L_g = & \int_0^L \frac{1}{2} M_o (1 + \eta x)^n \left(\frac{\partial w}{\partial t} \right)^2 dx + \frac{1}{2} M_c \left(\frac{\partial w(L_1)}{\partial t} \right)^2 \\
 & - \int_0^L \left[\frac{1}{2} EI_o (1 + \eta x)^{n+2} w_{,xx}^2 - \frac{1}{2} w_{,x}^2 (N_o (1 + \eta x)^{n+1}) \right] dx \\
 & + \frac{1}{2} m \left[\left(\frac{\partial w(L)}{\partial t} \right)^2 + 2l \left(\frac{\partial w(L)}{\partial t} \right) \left(\frac{\partial \theta}{\partial t} \right) \cos(\theta) + l^2 \left(\frac{\partial \theta}{\partial t} \right)^2 \right] \\
 & - mgl(1 - \cos(\theta)) - \frac{1}{2} K_p \theta^2
 \end{aligned} \tag{2.1}$$

where $w(L)$ is the displacement at the top of the tower, θ is the angle of the pendulum rotation, EI_0 is the flexural stiffness at the base of the column, N_0 , the normal force at the base, M_0 , the mass per unit length at the base, M_c , a concentrated mass at a distance L_1 from the base, L , the length of the column, m , the mass of the pendulum, K_p , the stiffness of the pendulum, l , the pendulum length and g is the acceleration of the gravity. Finally η and n are parameters that define the variation of the column cross-section. One can approximate by the suitable choice of η and n a large number of

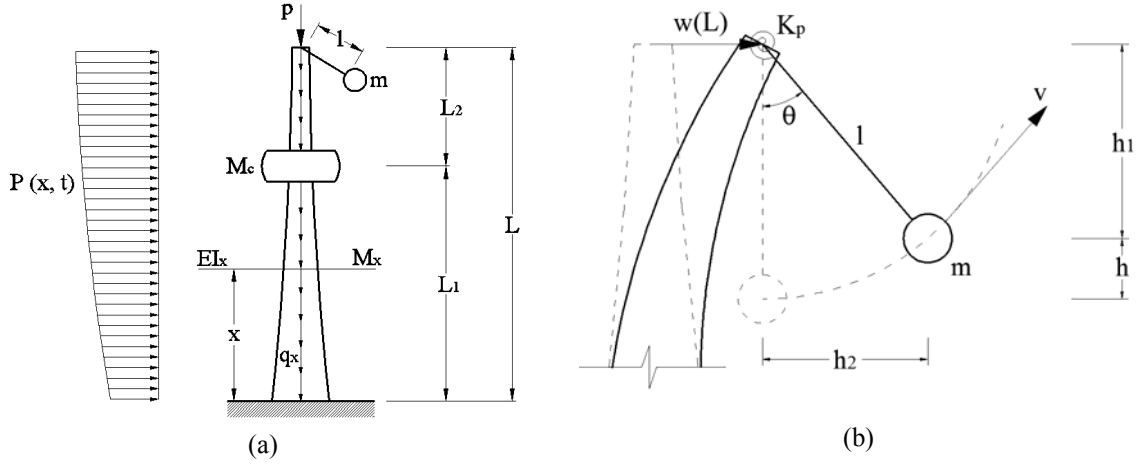


Fig. 1 Variable cross-section tower with a pendulum absorber: main parameters and reference system

column profiles found in practical applications (Korenev and Reznikov 1993, Qiusheng *et al.* 1994).

The nonlinear partial differential equations of motion for the column-pendulum system are obtained from Eq. (2.1) using the tools of variational calculus. They are

$$\frac{d^2}{dx^2} \left[EI_o (1 + \eta x)^{n+2} \left(\frac{\partial^2 w}{\partial x^2} \right) \right] + \frac{d}{dx} \left[N_o (1 + \eta x)^{n+1} \left(\frac{\partial w}{\partial x} \right) \right] + M_o (1 + \eta x)^n \left(\frac{\partial^2 w}{\partial t^2} \right) + M_c \delta(x - L_1) \left(\frac{\partial^2 w}{\partial t^2} \right) + m \delta(x - L) \left(\frac{\partial^2 w}{\partial t^2} \right) + \quad (2.2)$$

$$ml \delta(x - L) \left(\frac{d^2 \theta}{dt^2} \right) \cos(\theta) - ml \delta(x - L) \left(\frac{d\theta}{dt} \right)^2 \sin(\theta) = 0$$

$$ml^2 \left(\frac{d^2 \theta}{dt^2} \right) + K_p \theta + mgl \sin(\theta) + ml \delta(x - L) \left(\frac{\partial^2 w}{\partial t^2} \right) \cos(\theta) = 0 \quad (2.3)$$

where δ is the Dirac delta function.

3. Low dimensional model

To derive a consistent low dimensional model, a tower (without concentrated mass) with height $L = 360m$, cross sectional area $A = 2.97m^2$, mass per unit volume $\rho = 4176kg/m^3$, modulus of elasticity $E = 2.1 \times 10^{11}N/m^2$ and area moment of inertia $I = 133.61m^4$ is considered in the analysis. A pendulum with a mass $m = 44740kg$ (1.0% of the total mass of the column), length $l = 6.0m$ and $g = 9.81m/s^2$ is adopted. The pendulum is tuned to the lowest natural frequency of the tower (Korenev and Reznikov 1993, Den Hartog 1985). The lowest natural frequencies of the clamped-

free column is $\omega_c = 1.255 \text{ rad/s}$ and that of the pendulum is $\omega_p = \sqrt{g/l} = 1.279 \text{ rad/s}$. Considering a linear damped pendulum, the optimal damping of the pendulum is found to be 12% (Orlando 2006).

The column deflection can be approximated by the following series of orthogonal functions

$$f_b = \sum_{j=0}^b A_j \phi_j \quad (3.1)$$

where A_j are the time-dependent amplitudes and ϕ_j are the linear vibration modes of the column.

For the tower with variable cross section the vibration modes are given by (Orlando 2006)

$$\phi(x) = C_1 d_1^{-n} J_n(d_1) + C_2 d_1^{-n} Y_n(d_1) + C_3 d_2^{-n} I_n(d_2) + C_4 d_2^{-n} K_n(d_2) \quad (3.2)$$

where $J_n(d)$, $Y_n(d)$, $I_n(d)$ and $K_n(d)$ are Bessel functions of the n th order, and

$$d_1 = \frac{2}{\eta} \sqrt{N_e + \sqrt{N_e^2 + s^4} \sqrt{1 + \eta x}}, \quad d_2 = \frac{2}{\eta} \sqrt{N_e - \sqrt{N_e^2 + s^4} \sqrt{1 + \eta x}} \quad (3.3)$$

with $N_e = N_0/2EI_0$ and $s^4 = M_0 \omega_c^2/EI_0$.

For a column of constant cross section the eigenfunctions are

$$\phi(x) = C_1 \text{sen}(k_j x) + C_2 \text{cos}(k_j x) + C_3 \text{senh}(k_j x) + C_4 \text{cosh}(k_j x) \quad (3.4)$$

where, for a clamped-free column, k_j is the j th root of $2 + \cos(\beta_j) \cosh(\beta_j) = 0$ with $\beta_j = k_j L$.

The four lowest vibration modes and associated natural frequencies for the present example are shown in Fig. 2. As observed, the two lowest vibration frequencies are associated with the first tower flexural mode and pendulum mode, being the other natural frequencies much higher. If the analysis is restricted, as usual, to the lower frequency range, the pendulum-tower system can be approximated by a two d.o.f. model, as illustrated in Fig. 3 where d index denotes the modal properties. In Fig. 3, M_d , C_d and K_d are the modal mass, damping and stiffness coefficients associated with the first vibration mode, respectively, F_0 is the excitation magnitude and ω_e , the excitation frequency, while m_d and K_{pd} are, respectively, the mass and stiffness of the pendulum absorber and l_d , the pendulum length.

So, in the present work, first the free vibration modes and frequencies of the column (with and without concentrated masses) are obtained analytically using symbolic algebra. Then, these modes are used together with the Rayleigh-Ritz method to obtain the free vibration modes and frequencies of the column-pendulum system. Finally, a two degrees of freedom model, capable of describing with precision the behavior of the system in the neighborhood of the basic frequency of the column, is derived, from which the following set of nonlinear equations of motion, in non-dimensional form, is obtained

$$\begin{cases} (1 + \mu) \zeta_{,\tau\tau} + 2 \zeta_c \frac{\omega_c}{\omega_e} \zeta_{,\tau} + \left(\frac{\omega_c}{\omega_e} \right)^2 \zeta + \mu \theta_{,\tau\tau} \cos(\theta) - \mu \theta_{,\tau}^2 \sin(\theta) = \zeta_s \left(\frac{\omega_c}{\omega_e} \right)^2 \sin(\tau) \\ \mu \theta_{,\tau\tau} + 2 \mu \zeta_p \frac{\omega_p}{\omega_e} \theta_{,\tau} + \mu \zeta_{,\tau\tau} \cos(\theta) + \mu \left(\frac{\omega_p}{\omega_e} \right)^2 \sin(\theta) = 0 \end{cases} \quad (3.5)$$

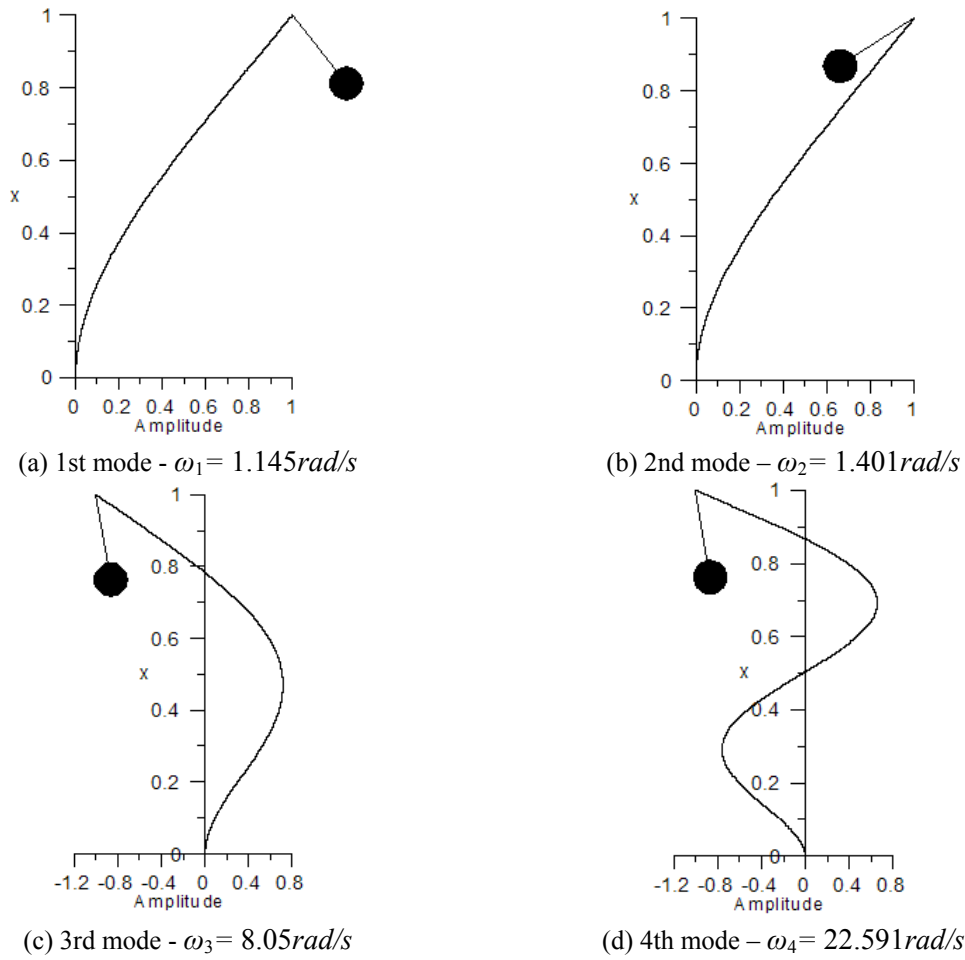


Fig. 2 Vibration modes and frequencies of the column-pendulum system $L = 360m$, $A = 2.97m^2$, $\rho = 4176 \text{ kg/m}^3$, $E = 2.1 \times 10^{11} \text{ N/m}^2$, $I = 133.61m^4$, $m = 44740 \text{ kg}$, $l = 6.0m$ and $g = 9.81 \text{ m/s}^2$

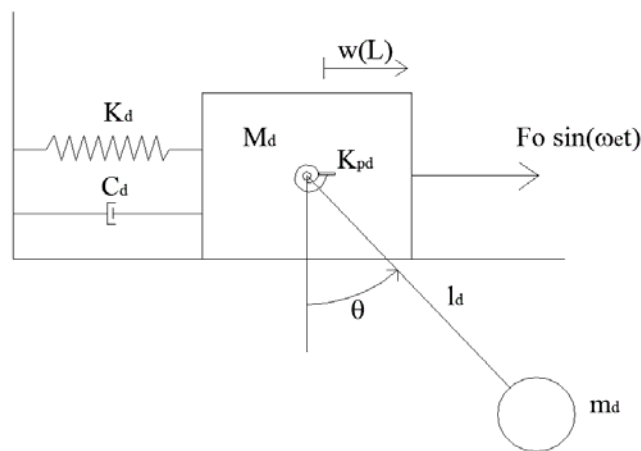


Fig. 3 Discrete 2dof mass-pendulum system

where $\zeta = w/L$, $\tau = \omega_e t$, is the nondimensional time parameter, ω_c is the natural frequency of the column; ζ_c is the damping ratio of the column; ω_p is the pendulum frequency, ζ_p is damping ratio of the pendulum absorber; μ is the mass ratio; ζ_s is the amplitude of the excitation force and ω_e is the excitation frequency.

The external control force is applied directly to the main structure in the opposite direction of the excitation force. It is given, in its non-dimensional form, as

$$Fc = f \tanh(\beta \zeta \zeta_{,\tau}) \zeta \quad (3.6)$$

being a function of the displacement and velocity of the column. The control force depends the parameters f and β and is a function of the tower displacement (ζ) and velocity ($\zeta_{,\tau}$). The use of \tanh function enables a smooth continuous variation of the nonlinear control force between the lower and upper values of the force ($\pm Fc$) and the parameter β controls the smoothness of this transition (see Fig. 9). In the literature usually the $\text{sign}(x)$ is usually used, but this represents an instantaneous change of the force (Winthrop *et al.* 2005, Leitmann 1994, Sonneborn and Van Vleck 1965), leading, in a nonlinear system, to a complex behavior (non-smooth system) and instabilities. A similar function is used to model magneto rheological dampers (Tang *et al.* 2004, Warminski and Kecik 2012).

Considering the external control force, the state equations are

$$\left\{ \begin{array}{l} \dot{y}_1 = y_2 \\ \dot{y}_2 = \left[\zeta_s \left(\frac{\omega_c}{\omega_e} \right)^2 \sin(\tau) - f \tanh(\beta y_1 y_2) y_1 - 2\zeta_c \frac{\omega_c}{\omega_e} y_2 - \left(\frac{\omega_c}{\omega_e} \right)^2 y_1 - \mu \dot{y}_4 \cos(y_3) + \mu y_4^2 \sin(y_3) \right] / (1 + \mu) \\ \dot{y}_3 = y_4 \\ \dot{y}_4 = -2\zeta_p \frac{\omega_p}{\omega_e} y_4 - \dot{y}_2 \cos(y_3) - \left(\frac{\omega_p}{\omega_e} \right)^2 \sin(y_3) \end{array} \right. \quad (3.7)$$

where $y_1 = \zeta$ is the displacement, $y_2 = \zeta_{,\tau}$ the velocity and $\dot{y}_2 = \zeta_{,\tau\tau}$ the acceleration of the column, and $y_3 = \theta$ is the displacement, $y_4 = \theta_{,\tau}$ the velocity and $\dot{y}_4 = \theta_{,\tau\tau}$ the acceleration of the pendulum absorber.

Although here, as in previous investigations (Wu *et al.* 2005, Winthrop *et al.* 2005, Azadi *et al.* 2009, 2011), the variable stiffness force has been applied to the main structure, to introduce the active force as an internal reaction force between the column and the pendulum in the hybrid case is also possible.

4. Nonlinear behavior of the column-pendulum system

First the nonlinear behavior of the tower-pendulum system is investigated. The main parameters of the system used in this investigation are: $\omega_c = 1.255 \text{ rad/s}$, $\zeta_c = 0.7\%$, $\zeta_p = 0.0\%$ (damping ratio of the pendulum is zero), $\mu = 0.04$ (4.0% of the modal mass of the first mode) and $\zeta_s = 0.007$ (amplitude of the excitation force).

There are three frequency parameters in Eq. (3.5): ω_c , the natural frequency of the column; ω_p , the pendulum frequency; and ω_e , the excitation frequency. The efficiency of the passive control systems depends on the relative values of these three parameters. Fig. 4 shows the variation of the

maximum steady-state amplitude of the tower with (continuous curve) and without (dashed line) the pendulum absorber as a function of ω_p for three different values of the ω_e/ω_c ratio, illustrating the three possible behavior of the absorber. For $\omega_e/\omega_c = 0.7965$ (Fig. 4(a)), that is, for $\omega_e < \omega_c$, the pendulum is effective only in the lower frequency range. For $\omega_p > 1$ the pendulum increases the maximum vibration amplitude as compared to that of the uncontrolled tower. Also, a significant decrease only occur around $\omega_p = 1.0$, when the vibration maximum amplitude approaches zero. If $\omega_e/\omega_c = 1.0$ (Fig. 4(b)), the pendulum is effective in the whole frequency range here analyzed, the maximum decrease of the column response occurs around $\omega_p = 1.2$. For $\omega_e/\omega_c = 1.1151$ (Fig. 4(c)), that is, for $\omega_e > \omega_c$, the behavior is just the opposite of that shown in Fig. 4(a) for $\omega_e < \omega_c$. So, the pendulum may increase or decrease the tower vibration amplitudes, depending on the forcing amplitude, which is unknown in practical applications, and the tuning of the pendulum-tower system. Several studies have shown that the nonlinearity of the pendulum play an important role on the vibrations of the tower, especially in extreme forcing cases, when the control system must be most effective (Mustafa and Ertas 1995, Warminski and Kecik 2009, Náprstek and Fischer 2009). On the other hand, the geometric nonlinearity of the tower has a negligible influence on the results (Orlando 2006).

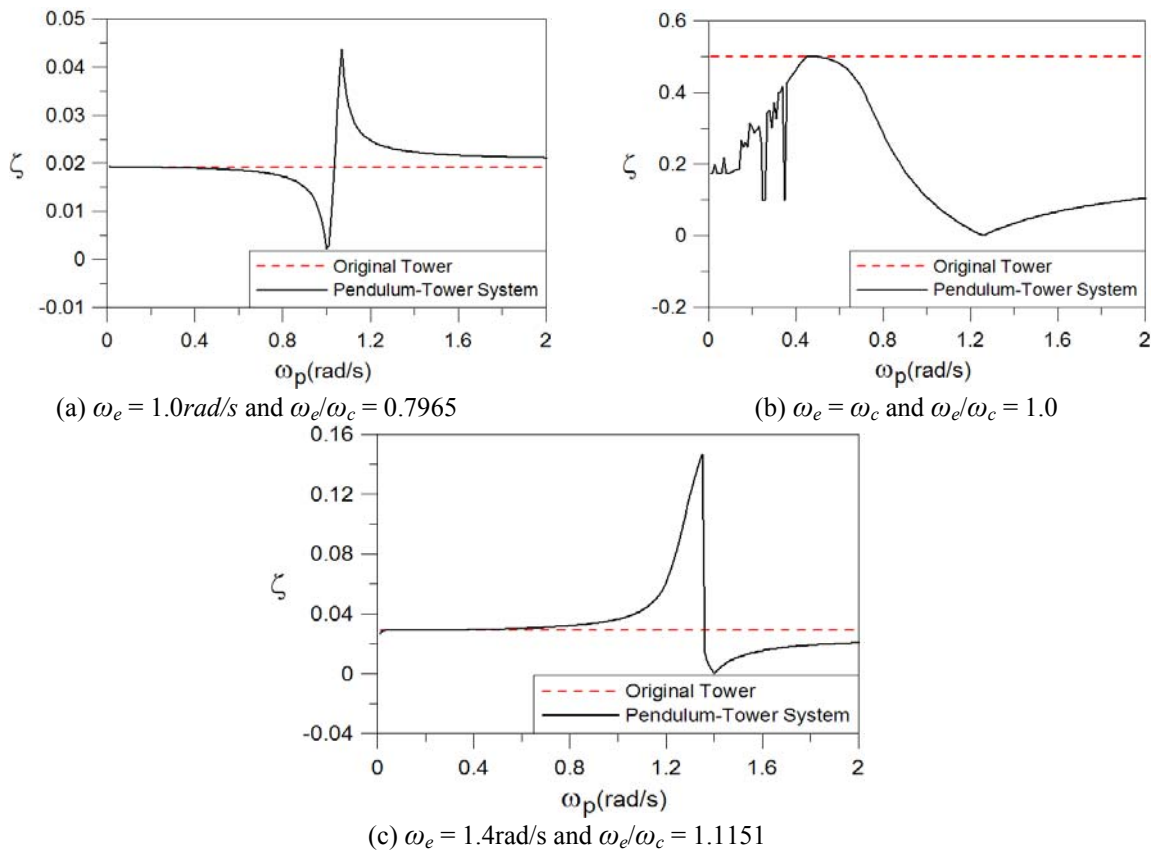


Fig. 4 Behavior of the maximum amplitude of displacement of the column in the permanent state. $\omega_c = 1.255 \text{ rad/s}$, $\zeta_c = 0.7\%$, $\zeta_p = 0.0\%$ (damping ratio of the pendulum is zero), $\mu = 0.04$ (4,0% of the modal mass of the first mode) and $\zeta_s = 0.007$ (amplitude of the excitation force)

Fig. 5 shows a comparison between the resonance curve of the tower and the pendulum, considering for the pendulum a linear and fully nonlinear modeling. It is clear that the consideration of a linear pendulum leads to an incomplete and incorrect evaluation of the pendulum damper on the maximum vibration amplitudes. The nonlinearity modifies the vibration amplitude and leads to a softening behavior with multiplicity of solutions and possible jumps between coexisting attractor in some frequency ranges. The results in Figs. 4 and 5 show that the pendulum nonlinearity may lead to complex dynamic behavior, depending on the relative values of the frequency parameters. Bifurcation diagrams of the Poincaré map as a function of ω_p for increasing values of the ω_e/ω_c ratio are shown in Fig. 6. The bifurcation diagrams are obtained by the numerical integration of the state Eq. (3.5) by the fourth order Runge-Kutta method together with the brute-force algorithm. Complex responses are detected, particularly for low values of ω_p . Some of these responses are illustrated in Figs. 7 and 8 where time responses, phase-plane responses and Poincaré sections are shown for, respectively, the column and the pendulum. While the tower shows nonlinear oscillations of different periods and quasi-periodic responses, as observed in the Poincaré maps, with small influence on the time response, the pendulum displays a complex oscillatory quasi-periodic behavior due to the influence of incommensurate frequencies. So, the trajectory is no longer closed, and the limit cycle becomes a limit torus.

These results show that the pendulum nonlinearity, although effective in reducing the frequency amplitudes in the main resonance region when properly tuned, may lead to unwanted complex solutions and jumps in an evolving dynamic environment. The response of the column-pendulum system can be improved and stabilized by adding to the structure some active control force, as shown in the next section.

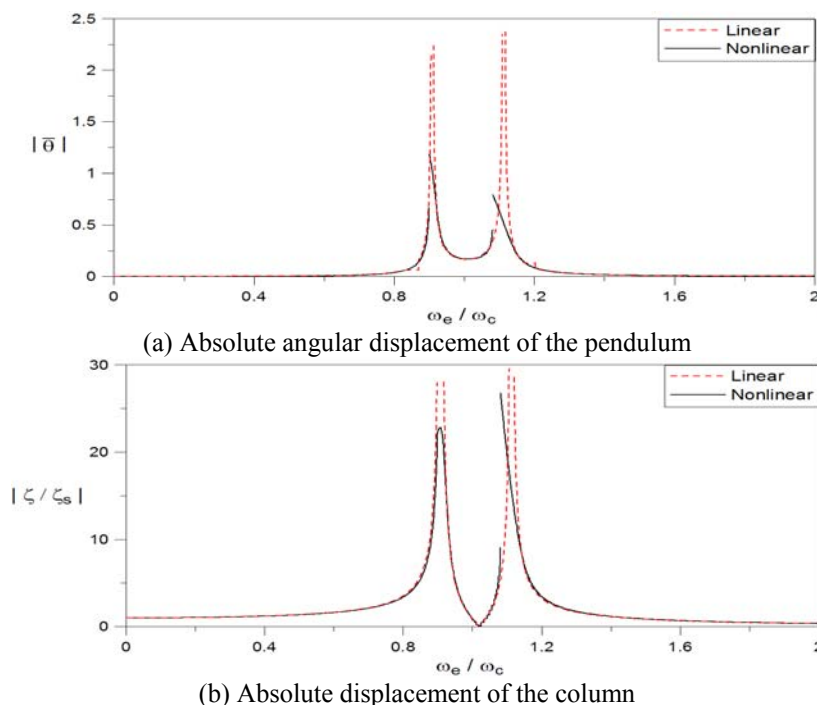


Fig. 5 Comparison of the response considering a linear and nonlinear pendulum model. The influence of the nonlinearity is observed in the main resonance regions. $\omega_p/\omega_c = 1.018$, $\omega_c = 1.255\text{rad/s}$, $\zeta_c = 0.7\%$, $\zeta_p = 0.0\%$, $\mu = 0.04$ and $\zeta_s = 0.007$

5. Hybrid control approach

To improve the effectiveness of the control during the transient response, a hybrid control system is suggested. The added control force is a non-linear variable stiffness device based on position and velocity feedback. The added force, as shown in Eq. (3.6), depends on two parameters, where f is the force magnitude and β controls the smoothness of the force in the transition zone. Fig. 9 shows the influence of parameter β on the control force ($x = \zeta \zeta_c$). As β

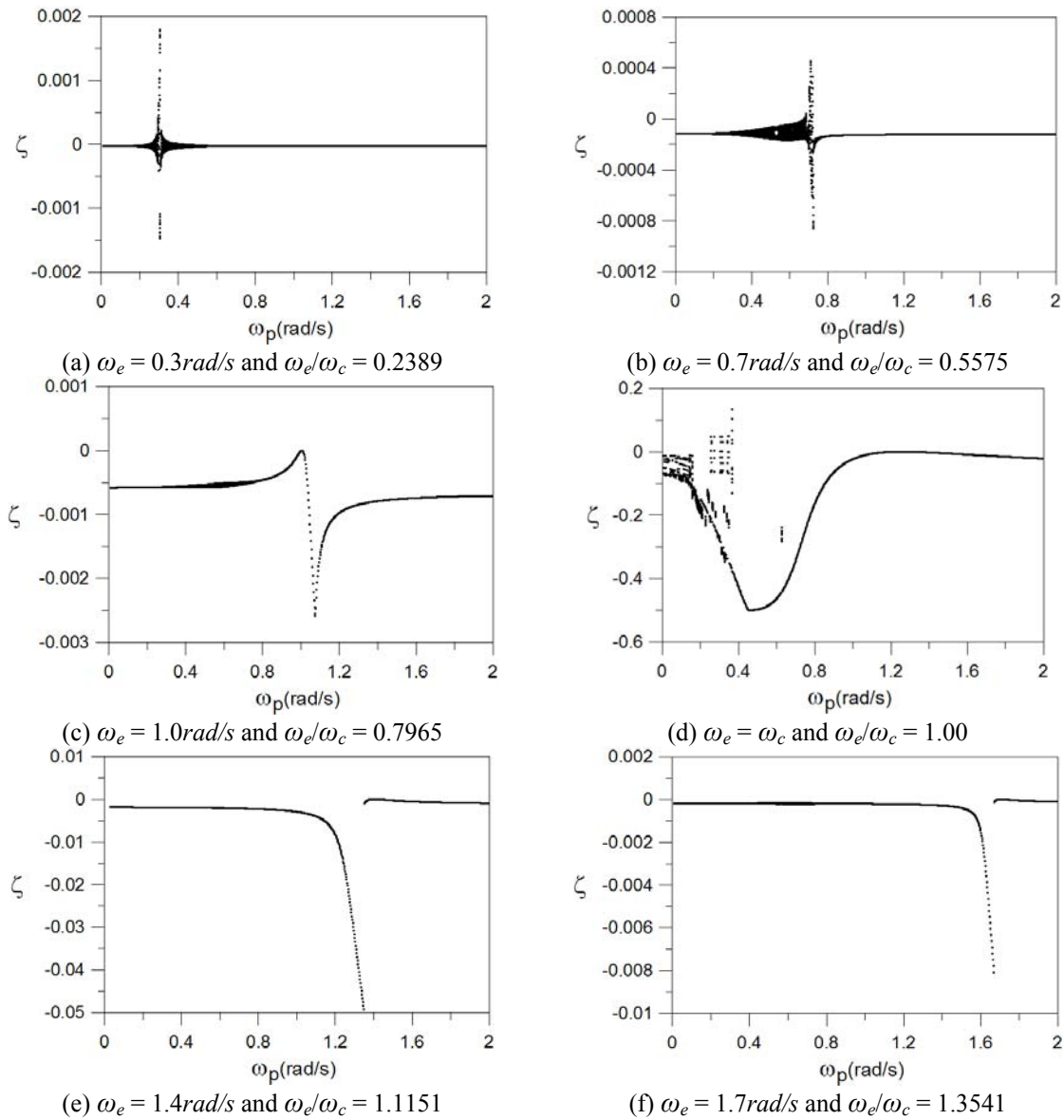


Fig. 6 Bifurcation diagrams of the Poincaré map. $\omega_c = 1.25 \text{ rad/s}$, $\zeta_c = 0.7\%$, $\zeta_p = 0.0\%$, $\mu = 0.04$ and $\zeta_s = 0.007$

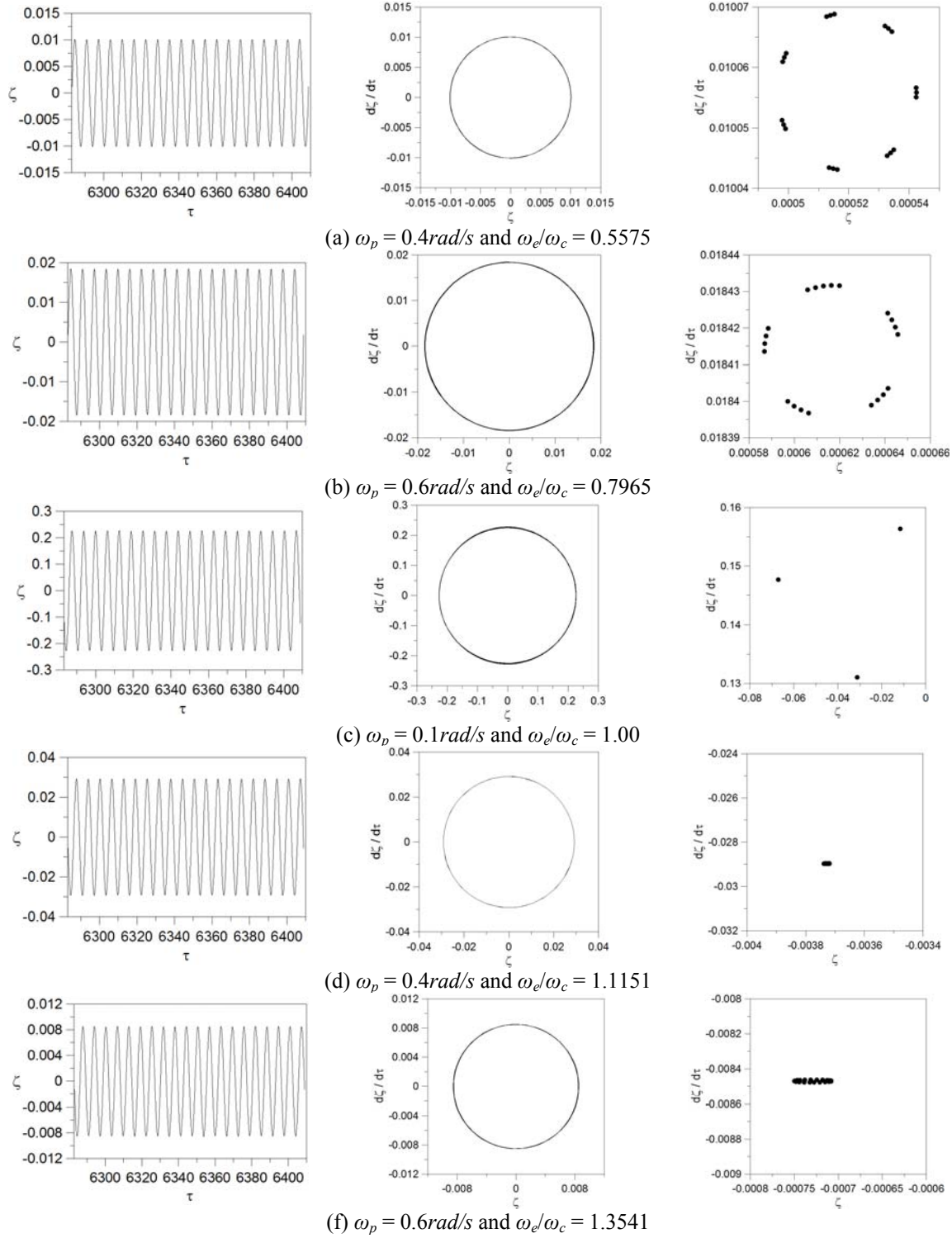


Fig. 7 Time response, phase plane and Poincaré map of the steady-state response of the tower. $\omega_c = 1.255\text{rad/s}$, $\zeta_c = 0.7\%$, $\zeta_p = 0.0\%$, $\mu = 0.04$ and $\zeta_s = 0.007$

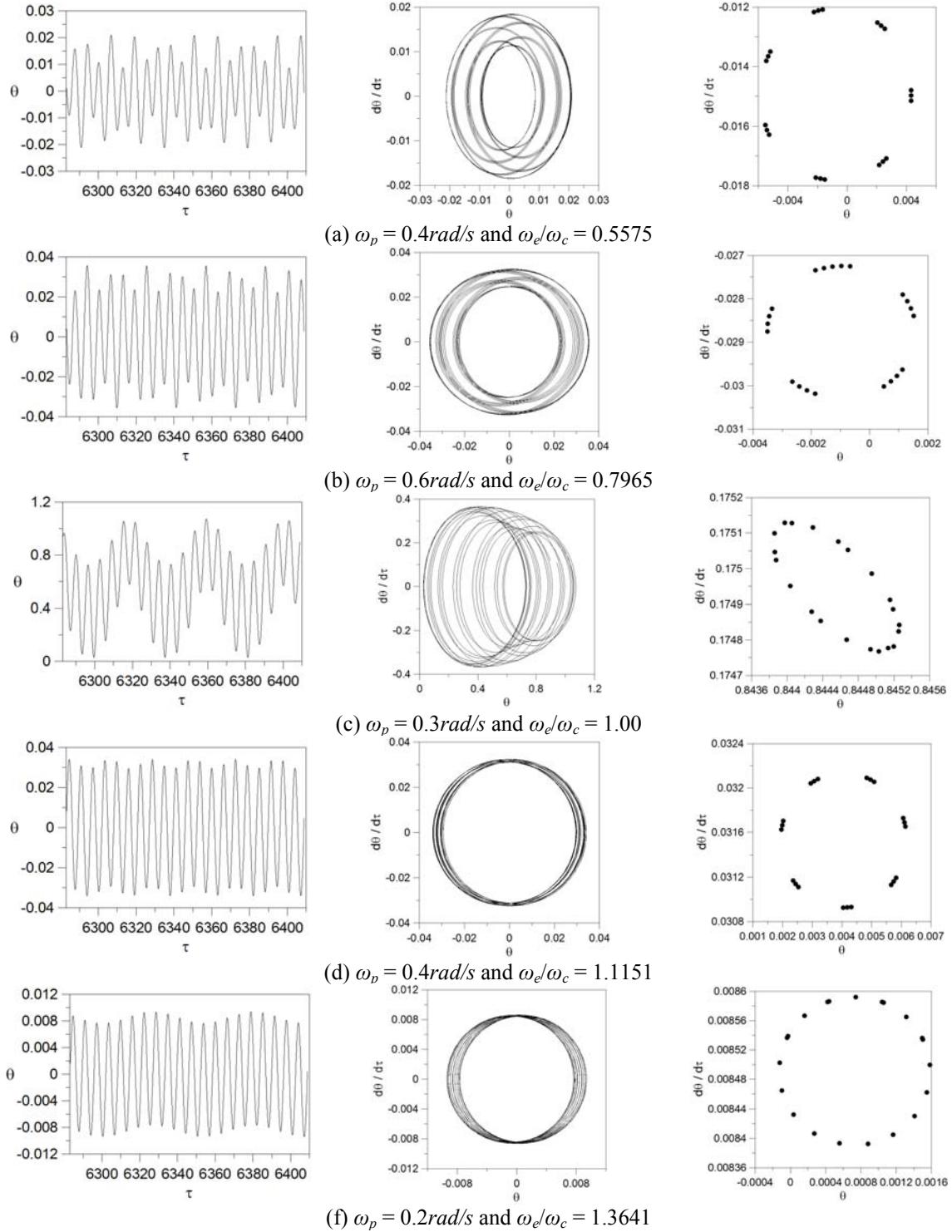


Fig. 8 Time response, phase plane and Poincaré map of the steady-state response of the pendulum. $\omega_c = 1.255 \text{ rad/s}$, $\zeta_c = 0.7\%$, $\zeta_p = 0.0\%$, $\mu = 0.04$ and $\zeta_s = 0.007$

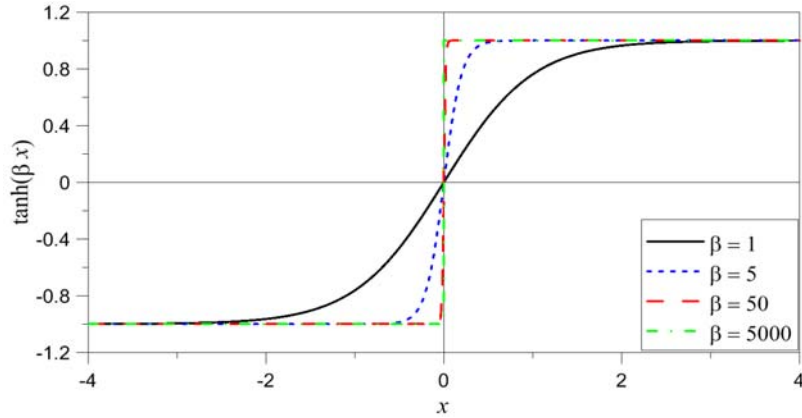


Fig. 9 Behavior of the function $\tanh(\beta x)$ for increasing values of β . $x = \zeta \zeta_\tau$

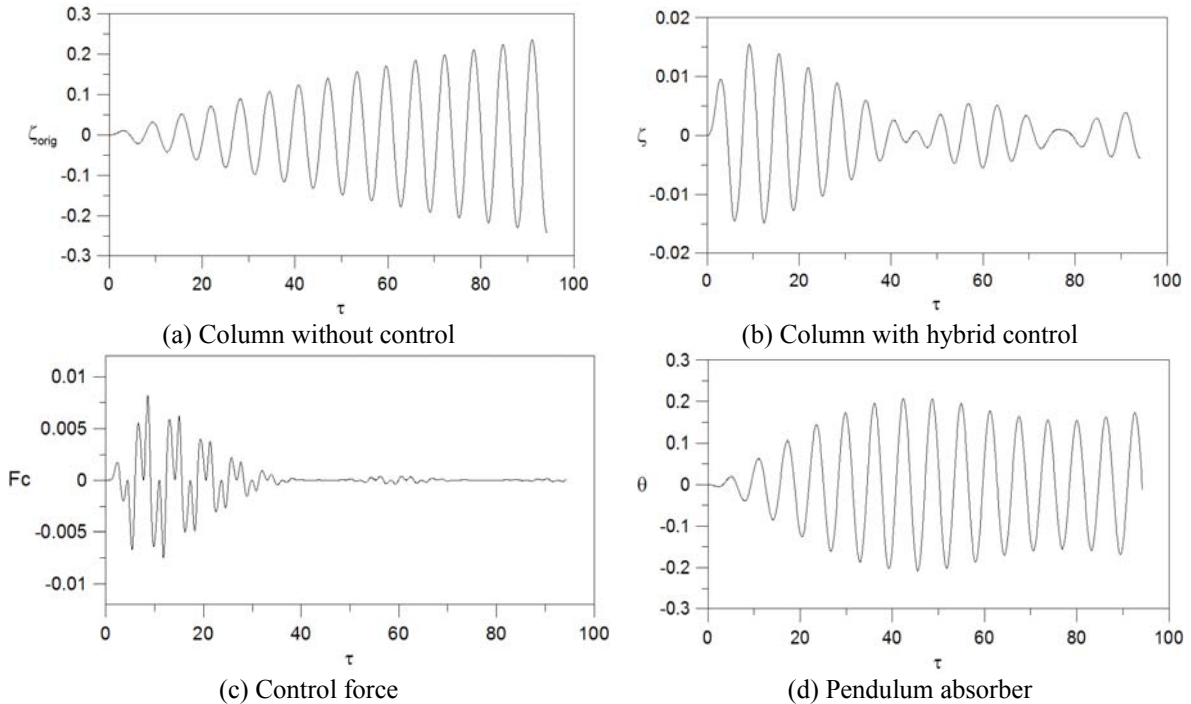


Fig. 10 Behavior of the system with hybrid control. $f = 1.0$, $\beta = 6000$, $\omega_c = \omega_p = \omega_e = 1.255 \text{ rad/s}$, $\xi_c = 0.07\%$, $\xi_p = 0.0\%$, $\mu = 0.04$ and $\zeta_s = 0.007$

increases, the force approach asymptotically the function $F_c = f \text{sign}(\zeta \zeta_\tau)$, when an abrupt change in the stiffness occurs (Winthrop *et al.* 2005, Leitmann 1994, Sonneborn and Van Vleck 1965). The latter function may lead to instability of the system in the presence of time delay. Also, in practical situations an instantaneous change of the sign of the force from $+f$ to $-f$ may not be possible. So, the description used in the present work seems to be more feasible and will lead to a more stable control system.

Fig. 10 clarifies the influence of the present control strategy on the behavior of the tower. Figs.

10(a) and 10(b) show, respectively, the uncontrolled and controlled response of the tower (maximum normalized displacement vs. time). A marked decrease in vibration amplitudes is obtained. The same is observed for velocities and accelerations. Fig. 10(c) shows the evolution of the control force, while Fig. 10(d) shows the response of the pendulum. First, while the response of the pendulum increases steadily from rest, the added control force acts to control the response of the tower but soon tends to zero as the pendulum reaches its full potential, absorbing most of the vibration energy. In this analysis is adopted $\omega_c = \omega_p = \omega_e = 1.255 \text{ rad/s}$, $\zeta_c = 0.7\%$, $\zeta_p = 0.0\%$, $\mu = 0.04$ and $\zeta_s = 0.007$, and the control force is computed considering $f = 1.00$ and $\beta = 6000$.

Table 1 shows, considering $\beta = 60$ and f varying from zero to two, the influence of the parameter f on maximum displacement, velocity and acceleration of the tower. It is observed that, as parameter f increases, the hybrid control becomes more efficient. However this increase is very small, which is an attractive aspect in a control mechanism, since a small force can be adopted leading to less energy consume. The maximum amplitude of the column in the steady-state regime is not affected by the variation of f . This is explained, as shown previously, by the fact that the pendulum is the responsible for the control of the vibrations in this phase, being the control force practically zero.

Now, the parameter β varies while the parameter f is taken equal to 1.00. Table 2 shows the behavior of the maximum displacement, velocity and acceleration of the column. As β increases the function $\tanh(\beta\zeta\zeta_r)$ tends asymptotically to the behavior of the function $\text{sign}(\zeta\zeta_r)$ and the efficiency of the control force increases markedly decreasing the maximum values that occur during the transient response. The amplitudes of the steady-state response are not altered by the value of β .

Fig. 11 shows a comparison of the steady-state response of the tower with passive and hybrid control for $\omega_c = \omega_p = 1.255 \text{ rad/s}$, $\zeta_c = 0.7\%$, $\zeta_p = 1.0$, $\mu = 0.04$, $\zeta_s = 0.007$, $f = 1.00$ and $\beta = 60$. The stable responses are represented by continuous lines, while the unstable responses are denoted by dotted lines. Comparing the two resonance curves, a strong decrease in the maximum vibration amplitude due to the hybrid control is observed. Also the hybrid control leads to the disappearance of the unstable branches.

To evaluate the efficiency of the hybrid control, results were also obtained for $\omega_e/\omega_c = 0.8991$ resulting in $\omega_e = 1.13 \text{ rad/s}$. This point, Fig. 12(a), coincides with the point where the absorber-tower system reaches the maximum amplitude. Fig. 12(b) shows a comparison of the tower and pendulum steady-state response with and without the active force. The results show that the hybrid control system practically eliminates the vibrations in the main resonance region of the coupled system.

In active, hybrid or adaptive control systems where feedback strategies are used, a certain amount of time is necessary to obtain and process the signal and, after that, evaluate and apply the control force. This time delay may cause a deterioration of the control system and can even cause instability (Liu *et al.* 2011). So, the influence of time delay is an essential step in the design of a given control system. Here the time delay, Td , is given as a percentage of the period of the tower response; T . Fig. 13 show the bifurcation diagram for a system without time delay and with a time delay equal to half of the period of the force, $Td = Tf/2$. It is observed that at the main resonance region the response becomes unstable. Based on these observations, a parametric analysis was conducted to evaluate the critical values of f and β as a function of the time delay. The results are presented in Figs. 14 and 15, where the variations of the critical values are shown as a function of the time delay. The worst case occurs when $Td/T = 0.5$. From the results, one can conclude that reasonable values of f and β can be used without instability problems due to time delay. However

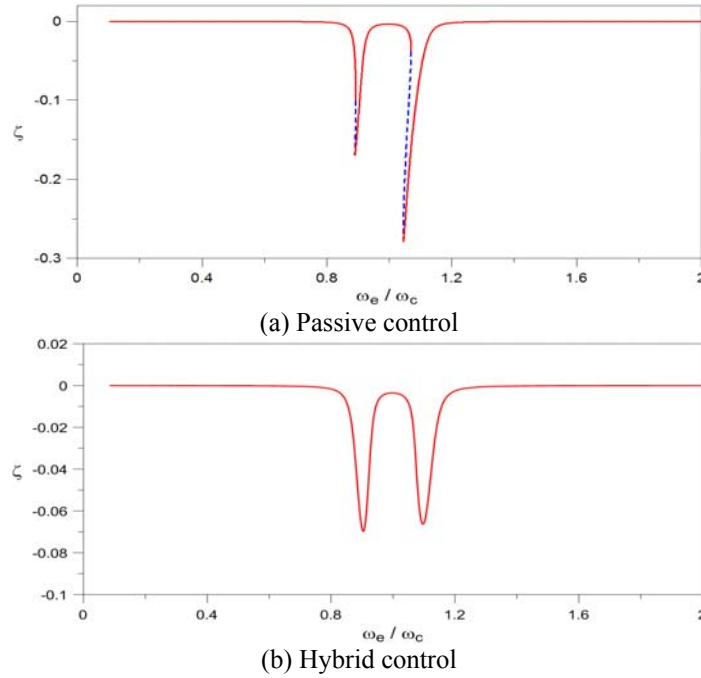


Fig. 11 Comparison of the steady-state response of the tower with passive and hybrid control for $\omega_c = \omega_p = 1.255rad/s$, $\zeta_c = 0.7\%$, $\zeta_p = 1.0\%$, $\zeta_s = 0.007$, $f = 1$ and $\beta = 60$. Continuous line – stable, dotted line – unstable

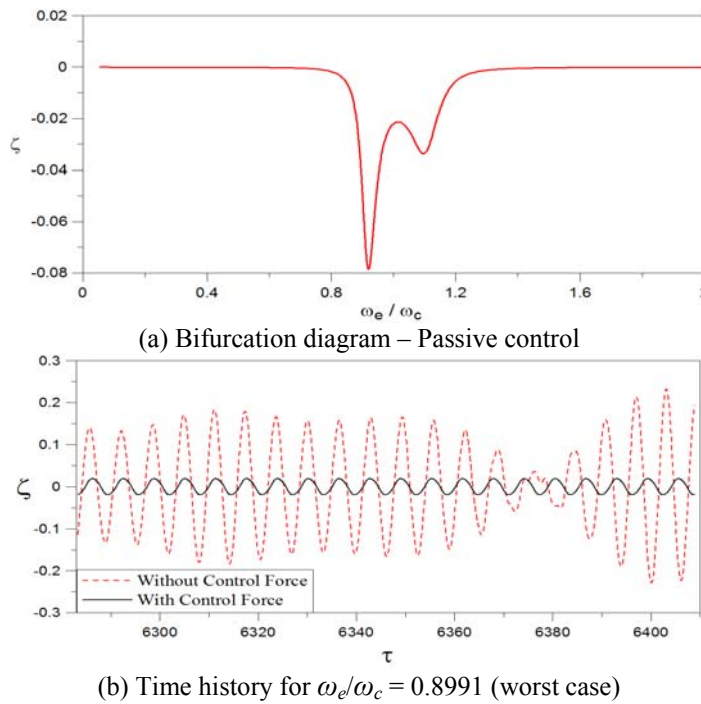


Fig. 12 Comparison of the amplitude of displacement with and without the control force. $f = 1$ and $\beta = 6000$, $\omega_c = 1.255rad/s$, $\omega_p / \omega_c = 1.018$, $\zeta_c = 0.7\%$, $\zeta_p = 7.0\%$ and $\zeta_s = 0.007$

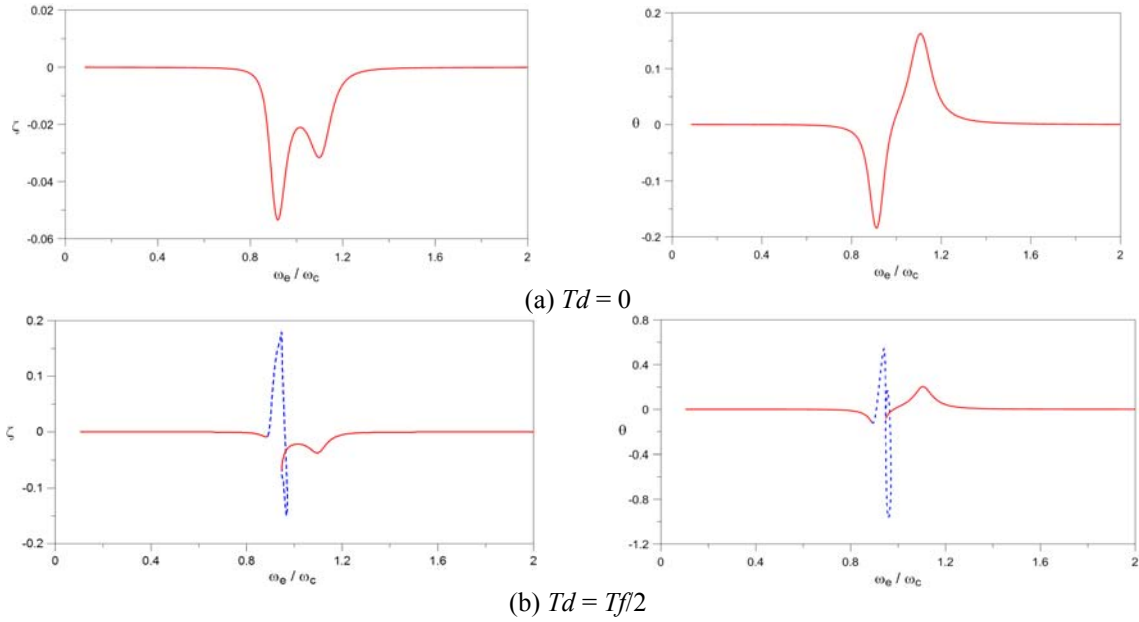


Fig. 13 Influence of time delay. $\omega_c = 1.255\text{rad/s}$, $\omega_p/\omega_c = 1.018$, $\zeta_c = 0.7\%$, $\zeta_p = 7.0\%$, $\zeta_s = 0.007$, $f = 1$, $\beta = 60$

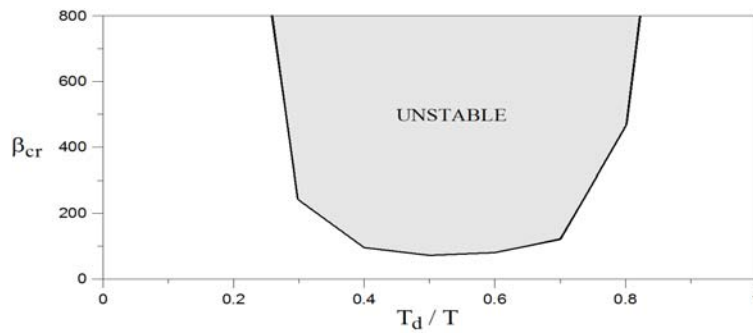


Fig. 14 Variation of the critical value of β as a function of time delay. $\omega_c = \omega_p = \omega_e = 1.255\text{rad/s}$, $\zeta_c = 0.7\%$, $\zeta_p = 0.7\%$, $\zeta_s = 0.007$ and $f = 1$

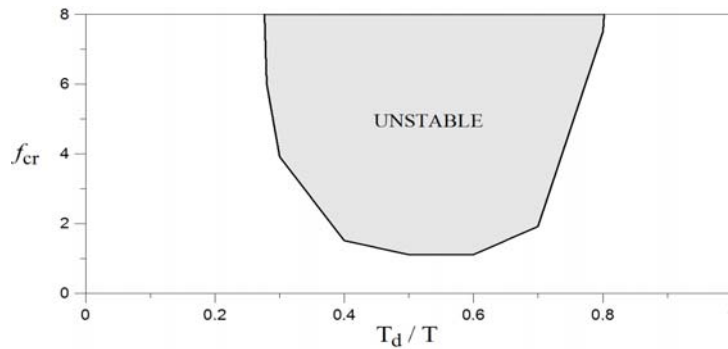


Fig. 15 Variation of the critical value of f as a function of time delay. $\omega_c = \omega_p = \omega_e = 1.255\text{rad/s}$, $\zeta_c = 0.7\%$, $\zeta_p = 0.0\%$, $\zeta_s = 0.007$ and $\beta = 60$

if higher values of f and β are required, several compensation methods including modifications of phase shift of the measured state variables in the modal domain and methods of updating the measured quantities can be found in literature (Soong 1988).

Based on the seminal ideas of Den Hartog (Den Hartog 1985, Korenev and Reznikov 1993, Soong and Dargush 1997), the optimal parameters of a tuned mass damper are usually obtained considering a harmonic excitation. This is rarely true in practical situations where loads do not lend themselves to explicit time description, being random or including at least some kind of noise. So it is important to know how departures from an ideally perfect harmonic excitation may affect the performance of a control device. Consider that the applied load is composed of an harmonic deterministic portion plus a random term, such that (Gonçalves and Santee 2008)

$$F_l(t) = F \cos(\Omega t) + G(t; F, \Omega) \quad (5.1)$$

where the random term $G(t; F, \Omega)$ depends the frequency Ω and amplitude F of the deterministic term and G has expected value zero, that is $E[G(t; F, \Omega)] = 0$.

The description of a stochastic process is usually made in the frequency domain. Here it is assumed that the random term has a spectral density function given by

$$\Phi_{GG}(\omega) = \frac{\sigma_{GG}^2}{2\omega_l} \quad \text{for} \quad \Omega - \frac{\omega_l}{2} < \omega < \Omega + \frac{\omega_l}{2} \quad (5.2)$$

where σ_{GG}^2 is the variance of the random force amplitude and ω_l is the frequency bandwidth. Additionally, it is considered that the standard deviation of the random force amplitude is proportional to the deterministic force amplitude, thus $\sigma_{GG} = aF$, where a is the standard deviation

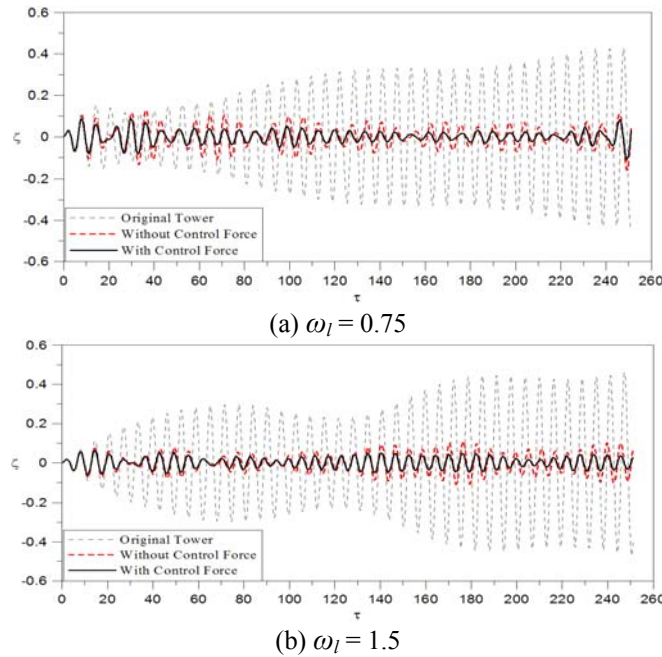


Fig. 16 Influence of random force. $\omega_c = \omega_p = \omega_e = 1.255 \text{ rad/s}$, $\zeta_c = 0.7\%$, $\zeta_p = 0.0\%$, $\zeta_s = 0.007$ and $f = 1$, $\beta = 60$ and $a = 0.3$

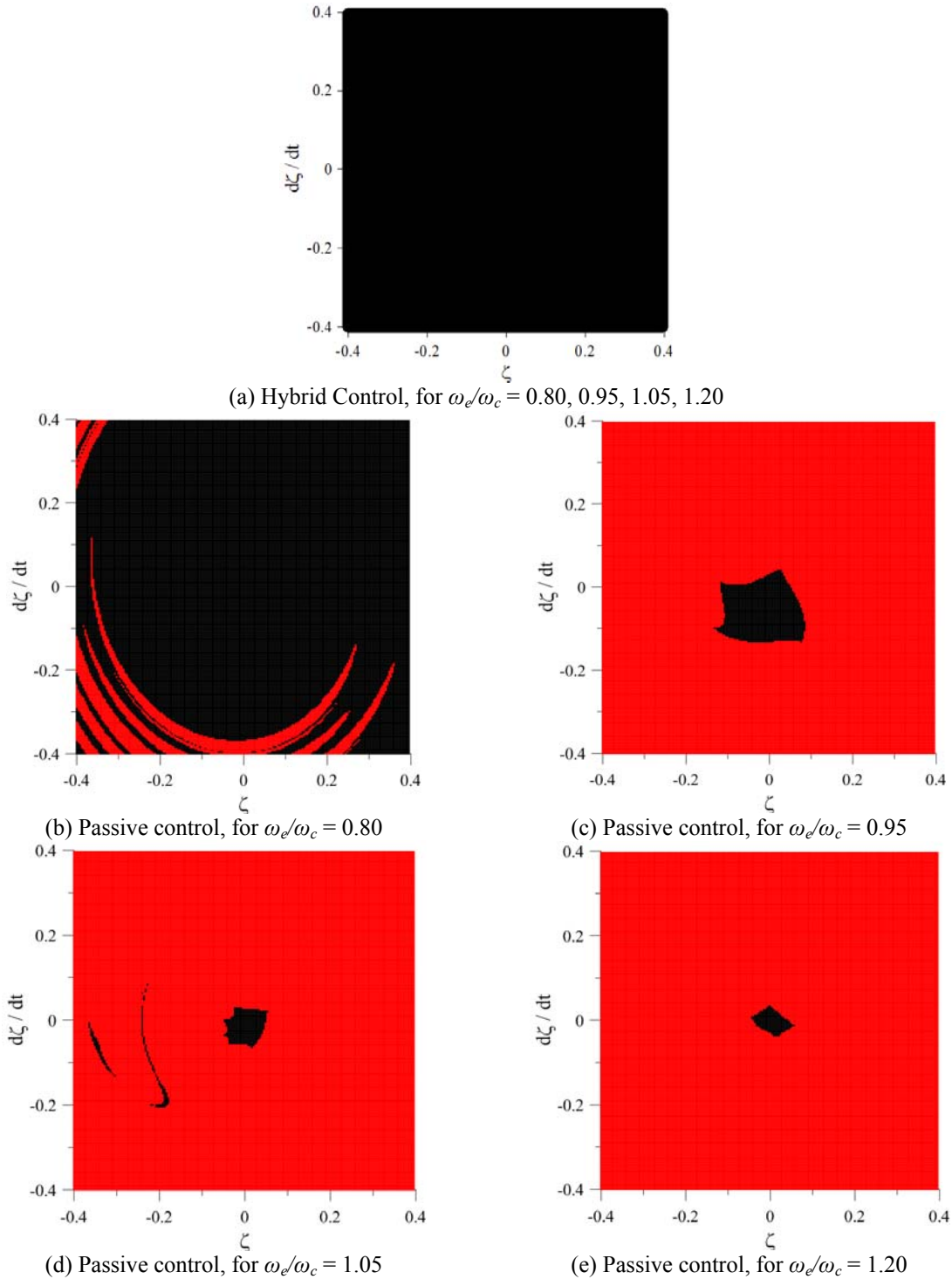


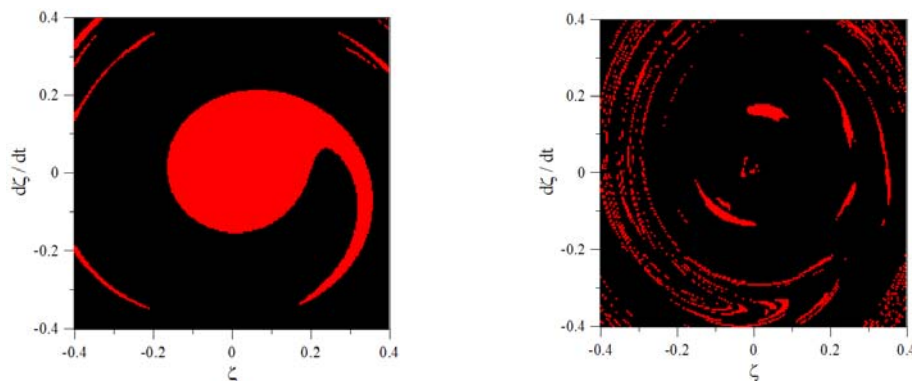
Fig. 17 Transient basins of attraction of the stable steady-state response. Number of forcing cycles necessary for the perturbed response converge to the fixed point of the Poincaré map. Black: 0-200, Red: 201-400 cycles. $\omega_c = \omega_p = 1.255 \text{ rad/s}$, $\zeta_c = 0.7\%$, $\zeta_p = 1.0\%$, $\zeta_s = 0.007$ and $f = 1$, $\beta = 60$

parameter. Two analyses considering $\omega_c = \omega_p = \omega_e = 1.255 \text{ rad/s}$, $\zeta_c = 0.7\%$, $\zeta_p = 0.0\%$, $\zeta_s = 0.007$, $f = 1$ and $\beta = 60$, are shown in Fig. 16 for two values of ω_l and $a = 0.3$. While the response of the uncontrolled tower exhibits large vibration amplitudes (dashed curve), the response of the tower-pendulum system exhibits a strong decrease of the vibration amplitudes of the tower response (red curve) which is further decreased by the addition of the variable stiffness device (black curve).

The evaluation of the safety and integrity of a nonlinear dynamical system is a subject of theoretical and practical importance in engineering. One way of investigating the dynamical integrity is through the analysis of the evolution of the basins of attraction of the various solutions. This issue was first addressed by Thompson and co-workers (Thompson 1989, Soliman and Thompson 1989). They introduced the concepts of safe basin and erosion profiles. This issue was further analyzed by several authors and nowadays it is agreed that the safety of a nonlinear mechanical system or structure depends not only on the stability of their solutions but also on the continuous and uncorrupted basin surrounding each solution, the total erosion of a given basin corresponding to the system failure (Rega and Lenci 2005). The integrity of a basin of attraction depends on the topology of the basin boundary, which can be smooth or fractal, and on the way that the basins of the various co-existing solutions interfere with each other (Soliman and Gonçalves 2003, Gonçalves *et al.* 2011).

Thompson and Soliman also introduced the concept of transient basin of attraction (Soliman and Thompson 1989, Soliman 1994). This tool can be used to measure the velocity with which a given attractor is approached and consequently the efficiency of a control system to damp the transient vibrations.

Fig. 17 shows the transient basins of attraction of the stable steady-state response of the tower with hybrid (Fig. 17(a)) and passive control. Each point in the basin of attraction corresponds to a set of two nonhomogeneous initial conditions of the tower (initial displacement field and velocity) thus accounting for a sudden application of the forcing or a sudden disturbance of the structure, leading to a transient response. The color scheme refers to the number of forcing period necessary to damp completely the transient response. As shown in Fig. 17(a), for the system with hybrid control all solutions converge to the desired attractor independent of the disturbance magnitude within 200 periods independent of the forcing frequency. For the passive case, the time



(a) $\omega_e/\omega_c = 1.05$. Black points, attractor $(-0.207, -0.231)$, Red points, attractor $(0, 0.013)$ (b) $\omega_e/\omega_c = 0.85$. Black points, attractor $(-0.002, 0.038)$, Red points, attractor $(-0.003, 0.038)$

Fig. 18 Basin of attraction – multiplicity of solution for the passive case. $\omega_c = \omega_p = 1.255 \text{ rad/s}$, $\zeta_c = 0.7\%$, $\zeta_e = 0.7\%$, $\zeta_p = 0.0\%$ and $\zeta_s = 0.007$

necessary to damp the transient response is much larger and depends on the value of the forcing frequency, as shown in Figs. 17(b)-17(e).

In the passive case, as already shown in Figs. 5 and 11, multiplicity of solutions may occur due to the nonlinearity of the resonance curves. Fig. 18 shows the basin of attraction for two cases where two competing solutions occurs (red and black basins). In Fig. 18(a) the basin boundary is smooth while in Fig. 18(b) the basin boundary is fractal. This leads to an uncertain outcome when the structure is subjected to a sudden disturbance and may lead to unwanted and even dangerous jumps between attractors in an evolving dynamic environment.

For the linear passive damper (Den Hartog 1985, Orlando 2006) it is found that a damping ratio of 12% leads to the optimal solution of the passive damper for the steady state response. However a high damping has a deleterious effect on the energy dissipation during the transient response. Considering the optimal value, $\zeta_p = 12.0\%$, Fig. 19 compare the transient basins of attraction of the stable steady-state response of the tower with hybrid and passive control. As in Fig. 17, each point corresponds to a set of initial conditions of the tower (initial displacement field and velocity), leading to a transient response. The color scheme refers to the number of forcing period necessary to damp completely the transient response. Fig. 19 shows that, even for this high damping level, the hybrid control display a more efficient performance on the rate of energy dissipation. This is

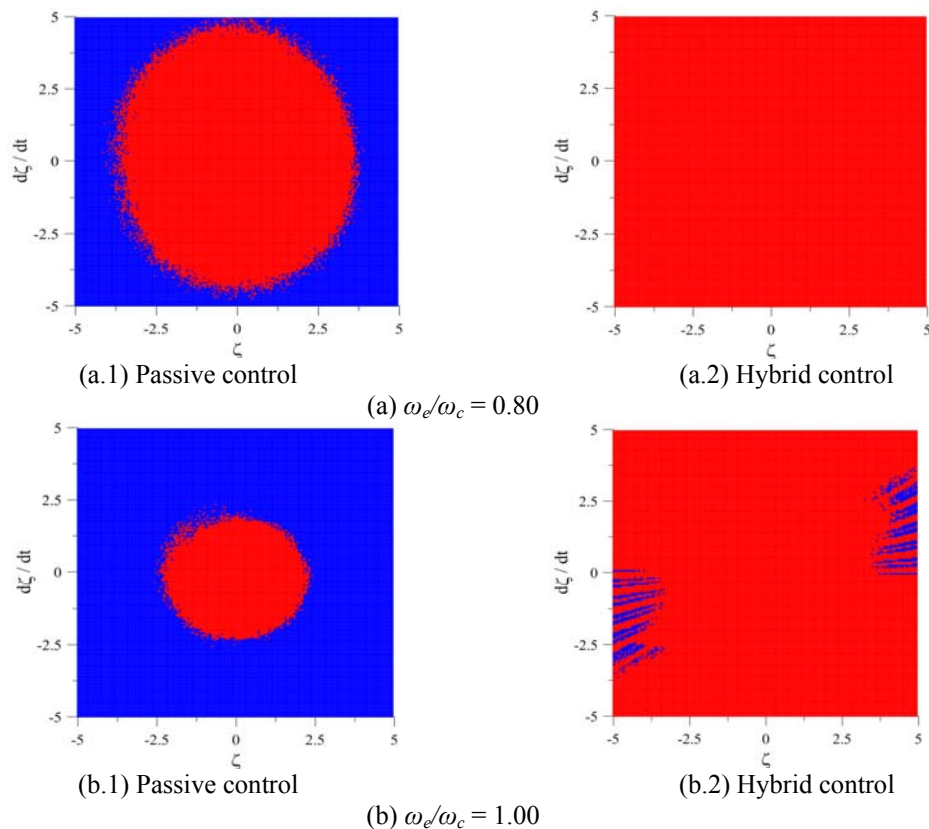


Fig. 19 Transient basins of attraction of the stable steady-state response. Number of forcing cycles necessary for the perturbed response converge to the fixed point of the Poincaré map. Black: 0-25, Red: 26-50, Blue: 51-75, Gray: 76-100. $\omega_c = \omega_p = 1.255rad/s$, $\zeta_c = 0.7\%$, $\zeta_p = 12.0\%$, $\zeta_s = 0.007$ and $f = 1$, $\beta = 60$

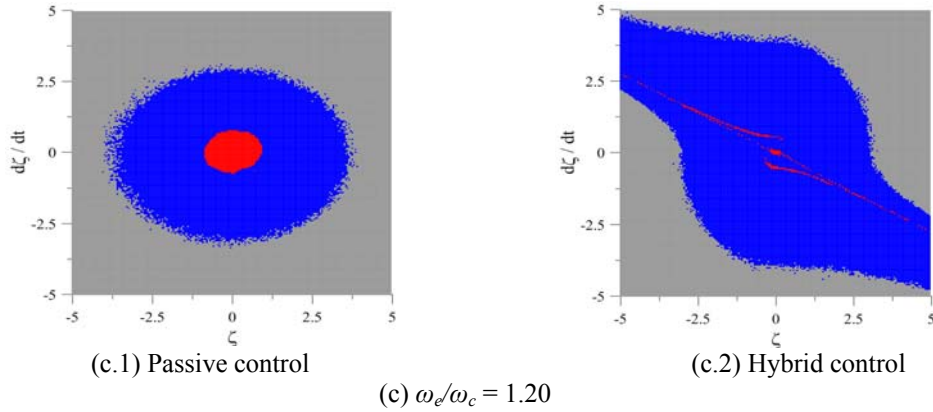


Fig. 19 Continued

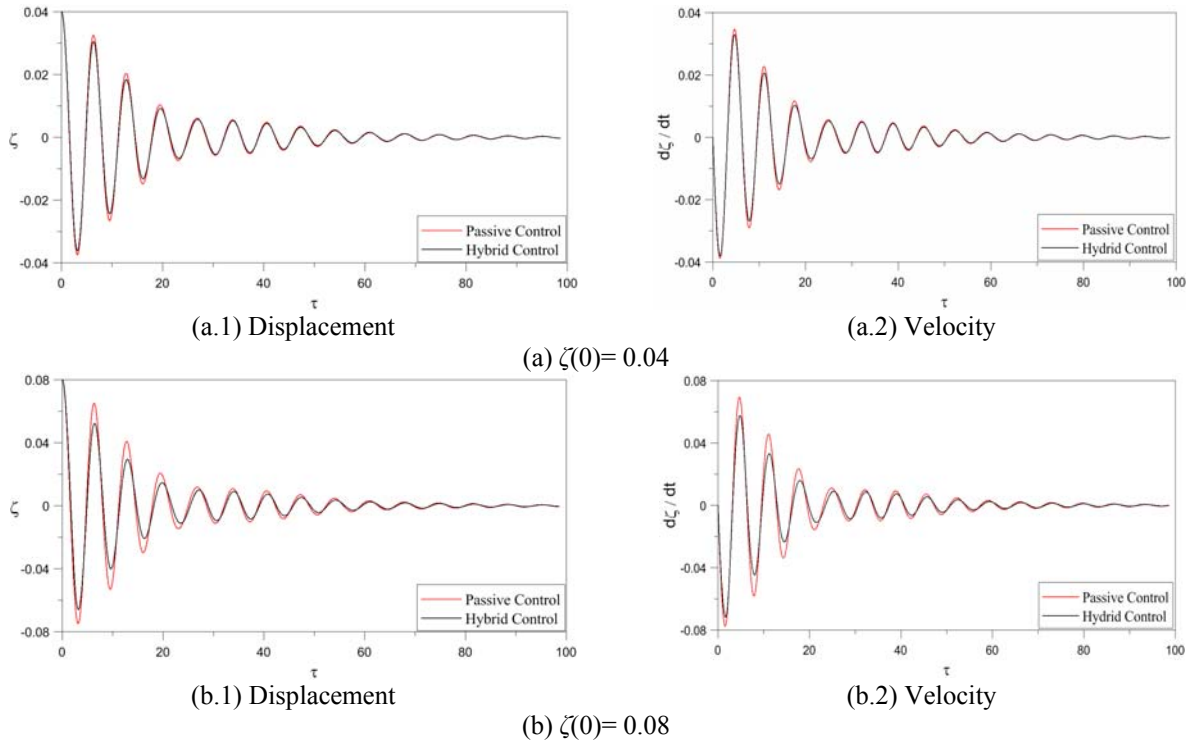


Fig. 20 Time history for $\omega_c = \omega_p = \omega_e = 1.255 \text{ rad/s}$, $\zeta_c = 0.7\%$, $\zeta_p = 12.0\%$, $\zeta_s = 0.0$ and $f = 1$, $\beta = 60$

also observed in Fig. 20, where the time responses of the tower displacement, $\zeta(\tau)$, and velocity, $\zeta_{,\tau}(\tau)$, considering a nonzero initial condition for the tower displacement, $\zeta(0)$, and both passive and hybrid control responses are compared.

Several devices have been proposed for the fabrication of variable stiffness springs in literature, including devices appropriate for tall buildings (Pneumatikos *et al.* 2004, Winthrop *et al.* 2005, Azadi *et al.* 2009, 2011, Rodriguez *et al.* 2011). To verify the numerical simulation results

experiments implementing the above control algorithm should be carried out. Although here, as in previous investigations (Wu *et al.* 2005, Winthrop *et al.* 2005, Azadi *et al.* 2009, 2011), the variable stiffness force has been applied to the main structure, to introduce the active force as an internal reaction force between the column and the pendulum mass in the hybrid case may be more feasible. The effectiveness of this alternative will be explored in a future work.

6. Conclusions

The analysis of a tall tower with a pendulum absorber was analyzed in the present work. The results show that the influence of the inertial and geometric nonlinearity of the pendulum cannot be disregarded in this class of problem. The results obtained without considering the damping of the pendulum present a strong nonlinearity of the softening type, where a decrease of the natural frequency with the vibration amplitude is observed, leading the sudden changes in vibration amplitudes. On the other hand, the nonlinearities decrease the vibration amplitudes in the resonance region during the steady-state response when compared with the usual linearized models. Although the increase of the damping of the pendulum improves the behavior of the system in the resonance region, it may be unfavorable during the transient regimen.

To improve the efficiency of the control, a hybrid control mechanism is proposed. Results demonstrate that the control force acts when the pendulum absorber starts to move. After the absorber reaches the amplitude necessary to control the oscillations of the column, the amplitude of the control force diminishes significantly. It is also observed that this control can practically eliminate the oscillations of the system in the main resonance region of the coupled pendulum-tower system. Results show that time delay has a major influence on the stability of the controlled response and that a proper choice of the active force parameters to avoid instability is an essential step in the control design. However additional studies and experimental analyses are necessary so that the efficiency of the proposed hybrid control can be properly evaluated.

Acknowledgments

The authors acknowledge the financial support of the Brazilian research agencies CAPES, FAPERJ and CNPq.

Reference

- Azadi, M., Behzadipour, S. and Faulkner, G. (2009), "Antagonistic variable stiffness elements", *Mechanism and Machine Theory*, **44**(9), 1746-1758.
- Azadi, M., Behzadipour, S. and Faulkner, G. (2011), "Performance analysis of a semi-active mount made by a new variable stiffness spring", *Journal of Sound and Vibration*, **330**(12), 2733-2746.
- Battista, R.C., Rodrigues, R.S. and Pfeil, M.S. (2003), "Dynamic behavior and stability of transmission line towers under wind forces", *Journal of Wind Engineering and Industrial Aerodynamics*, **91**(8), 1051-1067.
- Cicek, I. (2002), "Experimental investigation of beam-tip mass and pendulum system under random excitation", *Mechanical Systems and Signal Processing*, **16**(6), 1059-1072.
- Clark, W.W. (2000), "Vibration control with state-switched piezoelectric materials", *Journal of Intelligent Material Systems and Structures*, **11**(4), 263-271.

- Collette, F.S. (1998), "A combined tuned absorber and pendulum impact damper under random excitation", *Journal of Sound and Vibration*, **216**(2), 199-213.
- Den Hartog, J. P. (1985), *Mechanical Vibrations*, Dover Publications, NY.
- Ertas, A., Cuvalci, O. and Ekwaro-Osire, S. (2000), "Performance of pendulum absorber for a nonlinear system of varying orientation", *Journal of Sound and Vibration*, **229**(4), 913-933.
- Fischer, O. (2007), "Wind-excited vibrations-solution by passive dynamic vibration absorbers of different types", *Journal of Wind Engineering and Industrial Aerodynamics*, **95**, 1028-1039.
- Gerges, R.R. and Vickery, B.J. (2003), "Parametric experimental study of wire rope spring tuned mass dampers", *Journal of Wind Engineering and Industrial Aerodynamics*, **91**, 1363-1385.
- Gonçalves, P.B. and Orlando, D. (2007), "Influence of a pendulum absorber on the nonlinear behavior and instabilities of a tall tower", *IUTAM Symposium on Dynamics and Control of Nonlinear Systems with Uncertainty 2007*, Eds. H.Y. Hu and E. Kreuzer, Springer, The Netherlands.
- Gonçalves, P.B. and Santee, D. (2008), "Influence of uncertainties on the dynamic buckling loads of structures liable to asymmetric post-buckling behavior", *Mathematical Problems in Engineering*, doi:10.1155/2008/490137.
- Gonçalves, P.B., Silva, F.M.A., Rega, G. and Lenci, S. (2011), "Global dynamics and integrity of a two-dof model of a parametrically excited cylindrical shell," *Nonlinear Dynamics*, **63**, 61-82.
- Hassani, F.A., Payam A.F. and Fathipour, M. (2010), "Design of a smart MEMS accelerometer using nonlinear control principles", *Smart Structures and Systems* **6**, 1-16
- Korenev, B.G. and Reznikov, L.M. (1993), *Dynamic Vibration Absorbers: Theory and Technical Applications*, John Wiley & Sons, Chichester.
- Kourakis, I. (2007), "Structural systems and tuned mass dampers of super-tall buildings: case study of Taipei 101", Masters Thesis, Dept. of Civil and Environmental Engineering, Massachusetts Institute of Technology.
- Leitmann, G. (1994), "Semiactive control for vibration attenuation", *Journal of Intelligent Material Systems and Structures*, **5**, 841-846.
- Li, Q.S., Shang, G.Q., Huang, S.H. and Tuan, A.Y. (2011), "Wind-Induced Vibration Control of a Super-Tall Building with TMD", *Proceedings of the 13th International Conference on Wind Engineering*, Amsterdam.
- Liu, K., Chen, L.X., and Cai, G.P. (2011), "Active control of a nonlinear and hysteretic building structure with time delay", *Structural Engineering and Mechanics*, **40**(3), 431-451.
- Macias-Cundapi, L., Silva-Navarro, G. and Vázquez-Gonzalez, B. (2008), "Application of an Active Pendulum-Type Vibration Absorber for Duffing Systems", *Proceedings of the 5th International Conference on Electrical Engineering, Computing Science and Automatic Control (CCE 2008)* IEEE Catalog Number: CFP08827-CDR, ISBN: 978-1-4244-2499-3.
- Matta, E. and De Stefano, A. (2009), "Robust design of mass-uncertain rolling-pendulum TMDs for the seismic protection of buildings", *Mechanical Systems and Signal Processing*, **23**, 127-147.
- Mustafa, G. and Ertas, A. (1995), "Dynamics and Bifurcations of a Coupled Column-Pendulum Oscillator", *Journal of Sound and Vibration*, **182**(3), 393-413.
- Nagarajaiah, S. and Varadarajan, N. (2005), "Short time Fourier transform algorithm for wind response control of buildings with variable stiffness TMD", *Engineering Structures*, **27**, 431-441.
- Nagase, T. and Hisatoku, T. (1992), "Tuned-pendulum mass damper installed in crystal tower", *The Structural Design of Tall Buildings*, **1**, 35-56.
- Náprstek, J. and Fischer, C. (2009), "Auto-parametric semi-trivial and post-critical response of a spherical pendulum damper", *Computers and Structures*, **87**, 1204-1215.
- Nitzsche, F., Grewal, A. and Zimcik, D.G. (1999), "Structural component having means for actively varying its stiffness to control vibrations", *US patent 5*, 973, 440.
- Nitzsche, F., Zimcik, D.G., Wickramashinghe, V. and Chen, Y. (2004), "Control laws for an active tunable vibration absorber designed for rotor blade damping augmentation", *Aeronautical Journal*, **108**(1), 35-42.
- Orlando, D. (2006), "Pendulum Absorber for Vibration Control of Tall Towers", M.Sc. Dissertation, DEC – PUC-Rio, Rio de Janeiro, Brazil. (in Portuguese)

- Oueini, S.S., Nayfeh, H. and Pratt, J.R. (1999), "The Review of Development and Implementation of Active Non-Linear Vibration Absorber", *Archive of Applied Mechanics*, **69**, 585-620.
- Pneumatikos, N.K., Kallivokas, L.K., Gantes, C.J. (2004), "Feed-forward control of active variable stiffness systems for mitigating seismic hazard in structures", *Engineering Structures* **26**, 471-483.
- Pirner, M. (2002), "Actual behaviour of a ball vibration absorber", *Journal of Wind Engineering and Industrial Aerodynamics*, **90**, 987-1005.
- Qiusheng, L., Hong, C. and Guiqing, L. (1994), "Static and dynamic analysis of straight bars with variable cross-section", *Computers and Structures*, **59**, 1185-1191.
- Ramaratnam, A. and Jalili, N. (2006), "A switched stiffness approach for structural vibration control: theory and real-time implementation", *Journal of Sound and Vibration*, **291**, 258-274.
- Ramaratnam, A., Jalili, N. and Dawson, D.M. (2004), "Semi-active vibration control using piezoelectric-based switched stiffness", *Proceedings of American Control Conference*, Boston, MA.
- Rega, G. and Lenci, S. (2005), "Identifying, evaluating and controlling dynamical integrity measures in non-linear mechanical oscillators", *Nonlinear Analysis*, **63**, 902-914.
- Rodríguez, A.G., Chacón, J.M., Donoso, A. and Rodríguez, A.G.G. (2011), "Design of an adjustable-stiffness spring: Mathematical modeling and simulation, fabrication and experimental validation", *Mechanism and Machine Theory*, **46**, 1970-1979.
- Spencer, B. and Nagarajaiah, S. (2003), "State of the art of structural control", *J. Struct. Eng.*, **129**(7), 845-856.
- Soliman, M.S. (1994), "Global transient dynamics of nonlinear parametrically excited systems", *Nonlinear Dynamics*, **6**(3), 317-329.
- Soliman, M.S. and Gonçalves, P.B. (2003), "Chaotic behavior resulting in transient and steady state instabilities of pressure-loaded shallow spherical shells", *Journal of Sound and Vibration*, **259**, 497-512.
- Soliman, M.S. and Thompson, J.M.T. (1989), "Integrity measures quantifying the erosion of smooth and fractal basins of attraction", *Journal of Sound and Vibration*, **135**, 453-475.
- Sonneborn, L. and Van Vleck, F. (1965), "The bang-bang principle for linear control systems", *SIAM J. Control*, **2**, 151-159.
- Soong, Y.T. (1988), "State-of-the-art review: active control in civil engineering", *Eng. Struct.*, **10**, 74-83.
- Soong, T.T. and Dargush, G.F. (1997), *Energy Dissipation Systems in Structural Engineering*, John Wiley & Sons, Chichester.
- Tang, D., Gavin, H.P. and Dowell, E.H. (2004), "Study of airfoil gust response alleviation using an electromagnetic dry friction damper – part 1: theory", *Journal of Sound and Vibration*, **269**(20), 853-874.
- Thompson, J.M.T. (1989), "Chaotic behavior triggering the escape from a potential well", *Proc. Roy. Soc. London A*, **421**, 195-225.
- Vyas, A. and Bajaj, A.K. (2001), "Dynamics of autoparametric vibration absorbers using multiple pendulums", *Journal of Sound and Vibration*, **246**(1), 115-135.
- Warminski, J. and Kecik, K. (2009), "Instabilities in the main parametric resonance area of a mechanical system with a pendulum", *Journal of Sound and Vibration*, **322**, 612-628.
- Warminski, J. and Kecik, K. (2012), "Autoparametric vibrations of a nonlinear system with a pendulum and magnetorheological damping", *Nonlinear Dynamic Phenomena in Mechanics Solid Mechanics and Its Applications*, **181**, 1-61
- Winthrop, M.F., Baker, W.P. and Cobb, R.G. (2005), "A variable stiffness device selection and design tool for lightly damped structures", *Journal of Sound and Vibration*, **287**, 667-682.
- Wu, B., Liu, F.T. and Wei, D.M. (2005), "Approximate analysis method for interstorey shear forces in structures with active variable stiffness systems", *Journal of Sound and Vibration*, **286**, 963-980.
- Wu, S.T. (2009), "Active pendulum vibration absorbers with a spinning support", *Journal of Sound and Vibration*, **323**, 1-16.
- Wu, S.T., Chen, Y.R. and Wang, S.S. (2011), "Two-degree-of-freedom rotational-pendulum vibration absorbers", *Journal of Sound and Vibration*, **330**, 1052-1064.
- Yaman, M. and Sen, S. (2004), "The analysis of the orientation effect of non-linear flexible systems on performance of the pendulum absorber", *International Journal of Non-Linear Mechanics*, **39**, 741-752.